

# Circulation

JOURNAL OF THE AMERICAN HEART ASSOCIATION



## **Mouse Model of SCN5A-Linked Hereditary Lenègre's Disease: Age-Related Conduction Slowing and Myocardial Fibrosis**

Anne Royer, Toon A.B. van Veen, Sabrina Le Bouter, Céline Marionneau, Violaine Griol-Charhbili, Anne-Laure Léoni, Marja Steenman, Harold V.M. van Rijen, Sophie Demolombe, Catharine A. Goddard, Christine Richer, Brigitte Escoubet, Thérèse Jarry-Guichard, William H. Colledge, Daniel Gros, Jacques M.T. de Bakker, Andrew A. Grace, Denis Escande and Flavien Charpentier

*Circulation* 2005;111;1738-1746; originally published online Apr 4, 2005;

DOI: 10.1161/01.CIR.0000160853.19867.61

Circulation is published by the American Heart Association, 7272 Greenville Avenue, Dallas, TX 75214

Copyright © 2005 American Heart Association. All rights reserved. Print ISSN: 0009-7322. Online ISSN: 1524-4539

The online version of this article, along with updated information and services, is located on the World Wide Web at:

<http://circ.ahajournals.org/cgi/content/full/111/14/1738>

Subscriptions: Information about subscribing to *Circulation* is online at

<http://circ.ahajournals.org/subscriptions/>

Permissions: Permissions & Rights Desk, Lippincott Williams & Wilkins, a division of Wolters Kluwer Health, 351 West Camden Street, Baltimore, MD 21202-2436. Phone: 410-528-4050. Fax: 410-528-8550. E-mail:

[journalpermissions@lww.com](mailto:journalpermissions@lww.com)

Reprints: Information about reprints can be found online at

<http://www.lww.com/reprints>

## Mouse Model of *SCN5A*-Linked Hereditary Lenègre's Disease

### Age-Related Conduction Slowing and Myocardial Fibrosis

Anne Royer, PhD\*; Toon A.B. van Veen, PhD\*; Sabrina Le Bouter, PhD; Céline Marionneau, MSc; Violaine Griol-Charhbil, MSc; Anne-Laure Léoni, DVM; Marja Steenman, PhD; Harold V.M. van Rijen, PhD; Sophie Demolombe, PhD; Catharine A. Goddard, PhD; Christine Richer, PharmD, PhD; Brigitte Escoubet, MD, PhD; Thérèse Jarry-Guichard, PhD; William H. Colledge, PhD; Daniel Gros, PhD; Jacques M.T. de Bakker, PhD; Andrew A. Grace, PhD, FRCP; Denis Escande, MD, PhD; Flavien Charpentier, PhD

**Background**—We have previously linked hereditary progressive cardiac conduction defect (hereditary Lenègre's disease) to a loss-of-function mutation in the gene encoding the main cardiac Na<sup>+</sup> channel, *SCN5A*. In the present study, we investigated heterozygous *Scn5a*-knockout mice (*Scn5a*<sup>+/-</sup> mice) as a model for hereditary Lenègre's disease.

**Methods and Results**—In *Scn5a*<sup>+/-</sup> mice, surface ECG recordings showed age-related lengthening of the P-wave and PR- and QRS-interval duration, coinciding with previous observations in patients with Lenègre's disease. Old but not young *Scn5a*<sup>+/-</sup> mice showed extensive fibrosis of their ventricular myocardium, a feature not seen in wild-type animals. In old *Scn5a*<sup>+/-</sup> mice, fibrosis was accompanied by heterogeneous expression of connexin 43 and upregulation of hypertrophic markers, including  $\beta$ -MHC and skeletal  $\alpha$ -actin. Global connexin 43 expression as assessed with Western blots was similar to wild-type mice. Decreased connexin 40 expression was seen in the atria. Using pangenomic microarrays and real-time PCR, we identified in *Scn5a*<sup>+/-</sup> mice an age-related upregulation of genes encoding *Atf3* and *Egr1* transcription factors. Echocardiography and hemodynamic investigations demonstrated conserved cardiac function with aging and lack of ventricular hypertrophy.

**Conclusions**—We conclude that *Scn5a*<sup>+/-</sup> mice convincingly recapitulate the Lenègre's disease phenotype, including progressive impairment with aging of atrial and ventricular conduction associated with myocardial rearrangements and fibrosis. Our work provides the first demonstration that a monogenic ion channel defect can progressively lead to myocardial structural anomalies. (*Circulation*. 2005;111:1738-1746.)

**Key Words:** conduction ■ ion channels ■ remodeling

Idiopathic progressive cardiac conduction disease, also known as Lenègre or Lev's disease, is characterized by an age-related alteration in the conduction of the cardiac impulse that can ultimately lead to chronic atrioventricular block, justifying pacemaker implantation. Since the initial Lenègre and Lev's description,<sup>1,2</sup> it was considered a primary degenerative disease affecting the conducting network. In 1999, some of us identified a splicing mutation in the *SCN5A* gene in a French family, resulting in nonfunctional cardiac sodium channels and leading to hereditary Lenègre disease.<sup>3</sup> Interestingly, although the haploinsufficiency was already present

during infancy in the mutation carriers, the cardiac conduction defect worsened progressively with age, leading to life-threatening conduction blocks only in the older patients.<sup>4</sup> It was therefore likely that a combination between the *SCN5A* mutation and additional degenerative abnormalities in relation with aging explains the progressive alteration of the conduction velocity in hereditary Lenègre patients.

Most recently, a mouse model with targeted disruption of the *Scn5a* gene has been established.<sup>5</sup> Homozygous mice died before birth, whereas heterozygous (*Scn5a*<sup>+/-</sup>) mice survived and demonstrated conduction slowing qualitatively similar to

Received September 21, 2004; revision received November 30, 2004; accepted December 1, 2004.

From l'Institut du Thorax, INSERM U533 (A.R., S.L.B., C.M., A.-L.L., M.S., S.D., D.E., F.C.), Faculté de Médecine, Nantes, France; the Department of Medical Physiology (T.A.B.v.V., H.V.M.v.R.), University Medical Center, Utrecht, the Netherlands; the Experimental and Molecular Cardiology Group (J.M.T.d.B.), Academic Medical Center, Amsterdam, the Netherlands; the Section of Cardiovascular Biology (C.A.G., W.H.C., A.A.G.), Departments of Biochemistry and Physiology, University of Cambridge, Cambridge, UK; the Département de Pharmacologie (V.G.-C., C.R.), Faculté de Médecine Paris-Sud, Le Kremlin-Bicêtre, France; INSERM U426, CEFI IFR02 (B.E.), Université Paris 7, Paris, France; and CNRS UMR 6545, Institut de Biologie du Développement de Marseille (T.J.-G., D.G.), Université de la Méditerranée, Marseille, France.

\*The first 2 authors contributed equally to this work.

Correspondence to Flavien Charpentier, PhD, INSERM U533, Institut du Thorax, Faculté de Médecine, 1 rue G. Veil, 44035 Nantes cedex, France. E-mail flavien.charpentier@nantes.inserm.fr

© 2005 American Heart Association, Inc.

*Circulation* is available at <http://www.circulationaha.org>

DOI: 10.1161/01.CIR.0000160853.19867.61

that seen in inherited Lenègre patients. We thus decided to explore whether the *Scn5a*<sup>+/-</sup> mice undergo age-related changes in their cardiac phenotype, as do Lenègre patients. We found that the conduction defect in *Scn5a*<sup>+/-</sup> mice increases progressively with age and that this progression is associated with a pronounced myocardial rearrangement, including fibrosis and expression of hypertrophy markers but a conserved contractile function. Our data provide the first univocal demonstration that a monogenic ion channel defect can lead, with aging, to myocardial structural anomalies. Finally, by making use of a genetically engineered animal model, our results further support the original Lenègre and Lev's hypothesis suspecting a fibrotic process as being responsible for slowly progressing conduction defects.

## Methods

*Scn5a*<sup>+/-</sup> mice with 129/Sv genetic background were generated at the University of Cambridge (Cambridge, UK) and bred either at this institution or at l'Institut du Thorax (Nantes, France) and were genotyped by polymerase chain reaction (PCR) as previously described.<sup>5</sup> Because ECG studies revealed no phenotypic difference between the 2 sources of mice, data were pooled. The study conformed with the institutional guidelines for animal use in research. All experiments were performed on age-matched wild-type (WT) and heterozygous littermates.

## Electrocardiography

Three-lead ECGs were recorded with 25-gauge subcutaneous electrodes on a computer through an analog-digital converter (IOX 1.585, EMKA Technologies) for monitoring and later analysis (ECG Auto 1.5.7, EMKA Technologies). Recordings were filtered between 0.5 and 250 Hz. Mice were anesthetized with intraperitoneal injection of etomidate (15 mg/kg). Body temperature was maintained at 37°C by use of a thermally controlled heating pad (Harvard Apparatus). Criteria used for measuring RR, PR, QT<sub>r</sub>, and QT intervals (Figure 1), as well as P-wave duration, have been reported previously.<sup>6</sup> QT intervals were corrected for heart rate by use of the formula: corrected QT-interval duration (QT<sub>c</sub>) = QT/(RR/100)<sup>1/2</sup>, with QT and RR measured in milliseconds.<sup>7</sup> The QRS interval was measured from the beginning of the Q wave to the cross-point between the isoelectric line and the ST<sub>r</sub> segment (Figure 1).

## Echocardiography

Echocardiography was performed with a Toshiba Powervision 6000, SSA 370A device equipped with an 8- to 14-MHz linear transducer under isoflurane anesthesia (0.75% to 1.0% in oxygen) and spontaneous ventilation. Data were transferred to a computer for offline analysis (Ultrasound Image Workstation-300A, Toshiba). The left ventricle (LV) was imaged in parasternal long axis view for left atrium and LV measurement (end-diastolic diameter, ejection fraction, and shortening fraction) in time-motion mode. Pulse-wave Doppler tissue imaging was obtained from the posterior wall for the measurement of maximal wall velocities (systolic wave). The apical view was used for posterior wall Doppler measurement of LV mitral inflow (E wave) and LV aortic outflow (ejection time), as well as for tissue Doppler measurement of mitral annulus velocities (systolic wave and diastolic wave).

## Hemodynamics in Anesthetized Mice

Animals were anesthetized with intraperitoneal sodium pentobarbital (60 to 100 mg/kg), and the trachea was intubated to facilitate breathing. Body temperature was maintained at 37°C. The left jugular vein and the right carotid artery were isolated. A catheter tip pressure transducer (Mikrotip 1.4F, Millar Instruments) was inserted into the right carotid artery and advanced to the LV under guidance of the pressure signal and fixed in position. Blood pressure, heart rate, LV pressure, and maximal positive (+dP/dt) and maximal

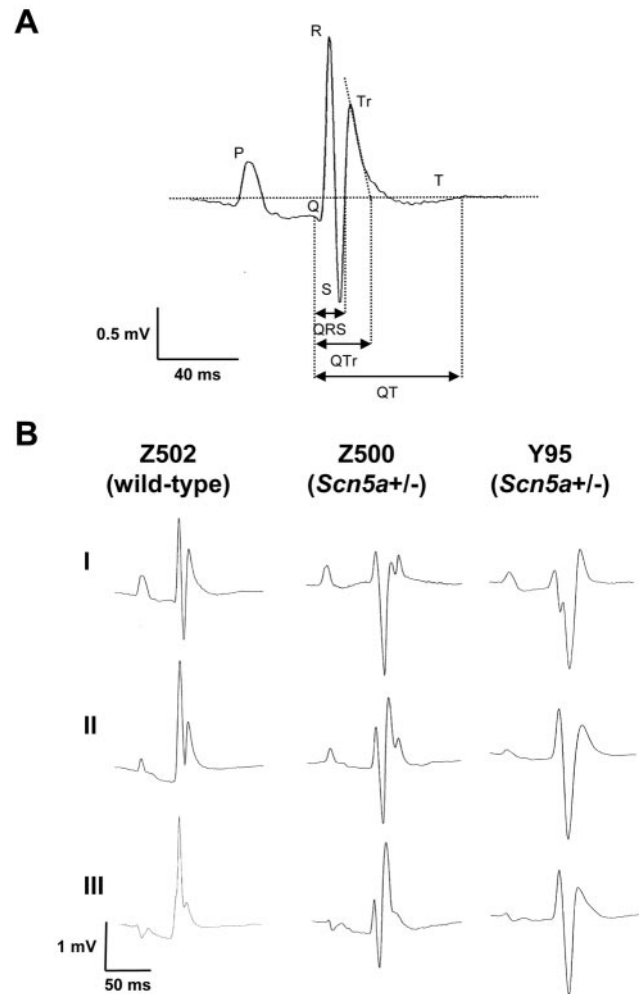


**Figure 1.** Surface ECGs in WT and *Scn5a*<sup>+/-</sup> mice. A, Method for measuring QRS, QT<sub>r</sub>, and QT intervals on mouse recordings (lead I). B, Representative ECG recordings (leads I, II, and III) in a WT and 2 different *Scn5a*<sup>+/-</sup> mice.

negative (-dP/dt) rates of pressure development were monitored for 10 minutes under basal conditions and during isoproterenol infusion (0.3 μg/mL at 1 μL · g<sup>-1</sup> · min<sup>-1</sup>, Abbott) on a computer with an MP100 system (Biopac Systems, Cerom).

## Real-Time RT-PCR

First-strand cDNA was synthesized from 2 μg of cardiac total RNA samples by use of high-capacity cDNA Archive Kit for reverse transcription (RT)-PCR (Applied Biosystems). Online PCR was performed with predesigned FAM-labeled fluorogenic TaqMan probes and primers and 1XTaqMan Universal Master Mix (Applied Biosystems). After 2 minutes at 50°C and 10 minutes at 95°C, 40 cycles of amplification were performed, each at 95°C for 15 seconds and 60°C for 1 minute, with the ABI PRISM 7900HT Sequence Detection System (Applied Biosystems). Data were collected with instrument-spectral compensation by the Applied Biosystems SDS 2.1 software. The fluorescence signals were normalized to the ubiquitously expressed housekeeping gene hypoxanthine guanine phosphoribosyl transferase (HPRT). The comparative threshold cycle relative quantification method<sup>8</sup> was used to compare the amounts of mRNA in WT and transgenic mice. Each plate contained duplicate quantification for each gene.

## Microarray Hybridization

Cy3- and Cy5-labeled cDNA was prepared from polyA<sup>+</sup> RNA samples by use of the CyScribe cDNA Post Labeling Kit (Amersham

**TABLE 1. ECG Characteristics of Wild-Type (n=85) and Heterozygous (*Scn5a*<sup>+/-</sup>; n=106) Mice**

	M/F	RR, ms	P, ms	PR, ms	QRS, ms	QTc	QTc	(QTc-QRS)c	(QT-QRS)c
Wild type	50/35	159±3	18±1	41±1	16±1	27±1	52±1	13±1	39±1
<i>Scn5a</i> <sup>+/-</sup>	60/46	170±2	21±1	45±1	24±1	30±1	58±1	11±1	40±1
<i>P</i> value vs wild type	NS	<0.01	<0.001	<0.001	<0.001	<0.001	<0.01	NS	NS

M/F indicates male/female ratio; RR, RR interval duration; P, P-wave duration; PR, PR-interval duration; QRS, QRS-complex duration; QTc, corrected QT interval duration; and NS, not significant.

The age of wild-type and *Scn5a*<sup>+/-</sup> mice ranged from 3 to 71 weeks, with average values of 18±2 and 21±2 weeks, respectively. Data are expressed as mean±SEM.

Pharmacia Biotech). Labeled samples were hybridized onto 2 MWG Mouse 10k Arrays according to the protocol provided by the manufacturer (MWG Biotech). Data were extracted as described previously.<sup>9</sup> Genes with Cy5/Cy3 expression ratios >1.5 or <0.67 in both 10k A or in both 10k B hybridizations were defined as differentially expressed.

### Immunohistochemistry and Histology

After excision, hearts were rapidly frozen in liquid nitrogen and stored at -80°C. For each group (young versus old and WT versus heterozygous), 5 hearts were serially sectioned to generate sections of 10-μm thickness. Sections taken from different levels were incubated with antibodies as reported previously.<sup>10</sup> After immunolabeling, sections were mounted in Vectashield (Vector Laboratories) and examined by use of a classic light microscope with epifluorescence equipment (Nikon Optiphot-2). To evaluate the presence of fibrosis, sections were fixed with 4% paraformaldehyde (in PBS, 30 minutes at room temperature) and stained with picosirius red.<sup>11</sup> Serial sections were stained with hematoxylin-eosin and analyzed with routine light microscopy.

### Protein Isolation, SDS-PAGE, and Western Blotting

Western blot experiments were performed with methods described previously.<sup>10,12</sup> For the experiments comparing young (14 to 16 weeks old) and old (50 to 73 weeks old) mice, total cellular protein was isolated from 5 hearts (total ventricular section) in each group (young versus old and WT versus *Scn5a*<sup>+/-</sup>) as described previously.<sup>10</sup> Protein content of the supernatant was assessed according to Lowry's method. Equal amounts (30 μg/lane) of each sample were separated on 10% SDS-polyacrylamide gels and transferred by electrophoresis to nitrocellulose membrane (Biorad). Equality of protein transfer was assessed by Ponceau S staining. After first and secondary horseradish peroxidase-conjugated antibody incubations, signals were visualized by use of an enhanced chemoluminescence reagent (Amersham) and exposure to XB-1 film (Kodak).

### Antibodies

The following antibodies were used: mouse monoclonal antibodies against connexin43 (Cx43; Transduction Laboratories), α-actinin (Sigma Aldrich), β-myosin heavy chain (β-MHC, kindly provided by Dr A.F.M. Moorman, Academic Medical Center, Amsterdam, the Netherlands) and desmin (Sigma Aldrich); rabbit polyclonal antibodies against Cx43 or connexin40 (Cx40),<sup>12</sup> N-cadherin (Sigma Aldrich), and skeletal α-actin (α-SKA, kindly provided by Dr S. Clement, University of Geneva, Switzerland). Secondary antibodies (Texas Red- and FITC-conjugated whole IgG) were purchased from Jackson Laboratories.

### Statistical Analysis

All data are expressed as mean±SEM. Statistical analysis was performed with a Fisher exact test, Student *t* test, and 1- or 2-way ANOVA completed by a Tukey test when appropriate. A value of *P*<0.05 was considered significant.

## Results

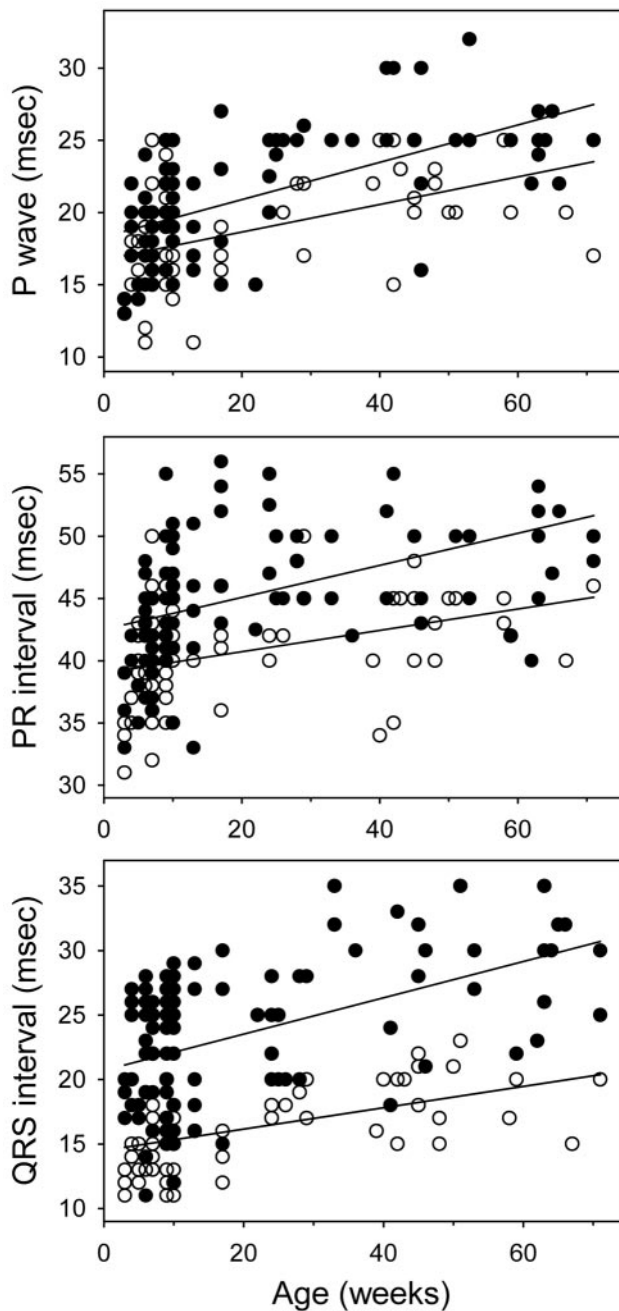
### Age-Related Progressive Development of the Conduction Defect in *Scn5a*<sup>+/-</sup> Mice

Figure 1B shows representative ECG recordings from a WT and 2 *Scn5a*<sup>+/-</sup> mice. Prolonged P-wave, PR-interval, and QRS interval durations (see Table 1 for average values from all mice studied) characterized *Scn5a*<sup>+/-</sup> mice. *Scn5a*<sup>+/-</sup> mice also showed slight but significant bradycardia, which was further confirmed by telemetry recordings (not illustrated). Figure 1B also shows that *Scn5a*<sup>+/-</sup> mice had a rightward shift in their cardiac axis. In contrast, the ventricular repolarization per se was not affected, because the observed prolongation in QTc and QTc intervals was caused by prolongation of the QRS interval (Table 1).

As shown in Figure 2, P-wave, PR, and QRS intervals progressively prolonged with aging (from 3 to 71 weeks; *P*<0.001 for all parameters). At every age range, these parameters were larger in *Scn5a*<sup>+/-</sup> than in WT mice (*P*<0.001 for all parameters). At the ventricular level, the progressive increase in QRS interval with aging was slightly although significantly more pronounced in *Scn5a*<sup>+/-</sup> than in WT mice. Indeed, the QRS/age slope was steeper in *Scn5a*<sup>+/-</sup> (0.14±0.02 ms/wk) than in WT animals (0.08±0.02 ms/wk; *P*<0.05). The observed age-related prolongation in conduction times coincided perfectly with our previous measurements in patients with genetically acquired Lenègre's disease (see Figure 5 in Reference 4).

### Age-Related Fibrosis in the Ventricular Myocardium of *Scn5a*<sup>+/-</sup> Mice

Ventricular sections stained with picosirius red were evaluated for the presence of fibrosis in young (14 to 16 weeks) and old (50 to 73 weeks) animals. Young mice, either WT or heterozygous, did not show fibrosis, with the exception of normal interstitial collagen between the muscle fibers (Figure 3A). The same pattern was found in old WT mice. In contrast, fibrosis in old *Scn5a*<sup>+/-</sup> mice was abundant and was found both in the left and right ventricular free walls and in the interventricular septum. The pattern of observed fibrosis was heterogeneous, with multiple spots of different sizes surrounded by healthy nonfibrotic myocardium. Typical examples of ventricular replacement fibrosis in old *Scn5a*<sup>+/-</sup> hearts are shown in Figure 3B. Both in the LV free wall and in the interventricular septum, staining of serial sections with hematoxylin shows that the fibrotic tissue was intermingled and surrounded by healthy myocardial bundles. Surprisingly, although in young *Scn5a*<sup>+/-</sup> mice, no fibrosis was observed in the ventricular working



**Figure 2.** Effects of age (x axis) on P-wave duration (y axis; top), PR interval duration (y axis; middle), and QRS interval duration (y axis; bottom) in WT (open symbols; n=106) and *Scn5a*<sup>+/-</sup> (filled symbols; n=85) mice.

myocardium, increased perivascular fibrosis could be detected, an anomaly not seen in young WT hearts (Figure 3C, left side). With aging, perivascular fibrosis became massive in *Scn5a*<sup>+/-</sup> mice (Figure 3C, right side). In areas of ventricular working myocardium where no fibrosis was detected (Figure 3D, area 1), a uniform expression pattern of the gap junction protein Cx43 was observed. In contrast, in areas of replacement fibrosis (Figure 3D, area 2), the uniform distribution was completely disturbed, because Cx43 could hardly be detected between myocytes within the scar, whereas its expression in the directly surrounding viable myocytes was irregular.

### Expression of Hypertrophic Markers in the Aged *Scn5a*<sup>+/-</sup> Myocardium

Immunolabeling with antibodies against the hypertrophic markers  $\beta$ -MHC and skeletal  $\alpha$ -actin was used to evaluate the status of the ventricular myocardium (Figure 4A). The expression of these structural proteins is very low in the healthy mouse heart but is upregulated in myopathological conditions. In the heart of young WT mice, rare areas with immunopositive cells were found. The amount of positive areas and the intensity of labeling were slightly increased in young *Scn5a*<sup>+/-</sup> mice. In contrast, a large increase in immunolabeled cells was observed in the myocardium of old *Scn5a*<sup>+/-</sup> animals. Western blots incubated with antibodies against skeletal  $\alpha$ -actin confirmed this increased expression (Figure 4B). Antibodies against  $\beta$ -MHC were found to be ineffective on Western blot. Figure 4 also shows the expression level of  $\alpha$ -actinin. This protein of the contractile machinery is expressed primarily in the normal myocardium. In young animals,  $\alpha$ -actinin was equally expressed in the ventricle of WT and *Scn5a*<sup>+/-</sup> animals. In old mice, however,  $\alpha$ -actinin was expressed at a substantially higher level in the *Scn5a*<sup>+/-</sup> hearts. At the mRNA level, real-time RT-PCR experiments confirmed the age-dependent increase in  $\beta$ -MHC and skeletal  $\alpha$ -actin expression in *Scn5a*<sup>+/-</sup> mice. Whereas  $\beta$ -MHC expression was normal in 10-week-old *Scn5a*<sup>+/-</sup> mice ( $0 \pm 7\%$  versus WT; n=12), it was upregulated by  $46 \pm 15\%$  and  $70 \pm 21\%$  in 21-week-old (n=12) and 56- to 60-week-old (n=12) animals, respectively. Similar observations were obtained with skeletal  $\alpha$ -actin. In contrast, the expression of troponin I mRNA was unaltered.

We used mouse pangenomic microarrays (20 000 oligonucleotides) to characterize further the cardiac gene expression remodeling in *Scn5a*<sup>+/-</sup> mice. For this, two 11-month-old *Scn5a*<sup>+/-</sup> mice were compared with 2 age-matched WT mice. The list of genes differentially expressed in *Scn5a*<sup>+/-</sup> mice (as defined in the Methods section) can be found at <http://www.nantes.inserm.fr/u533/INDEX/>. Among the genes found to be upregulated, 2 were of particular interest and were characterized further with real-time RT-PCR: the early growth response 1 (*Egr1*) and activating transcription factor 3 (*Atf3*) genes (Figure 4C). The expression of both transcription factors was comparable in WT and *Scn5a*<sup>+/-</sup> young (10-week-old) animals but consistently increased with aging in *Scn5a*<sup>+/-</sup> mice.

### Remodeling of Gap Junction Protein Expression

Western blot experiments indicated that the expression of Cx43 protein in the ventricles or atria of both 30- to 40-week-old WT and *Scn5a*<sup>+/-</sup> mice was similar (Figure 5A). In contrast, the expression of Cx40 was reduced by approximately 50% in the atria of *Scn5a*<sup>+/-</sup> compared with WT mice. We observed that the regional distribution of Cx43 in the ventricle of *Scn5a*<sup>+/-</sup> old animals was markedly disturbed because of heterogeneously located patches of fibrosis (see Figure 3D). Further Western blots were thus performed in young (14- to 16-week-old) and old (50- to 73-week-old) mice with a different antibody. Results confirmed that the ventricular expression of Cx43 was similar in both WT and *Scn5a*<sup>+/-</sup> mice, even in older animals (Figure 5B). We

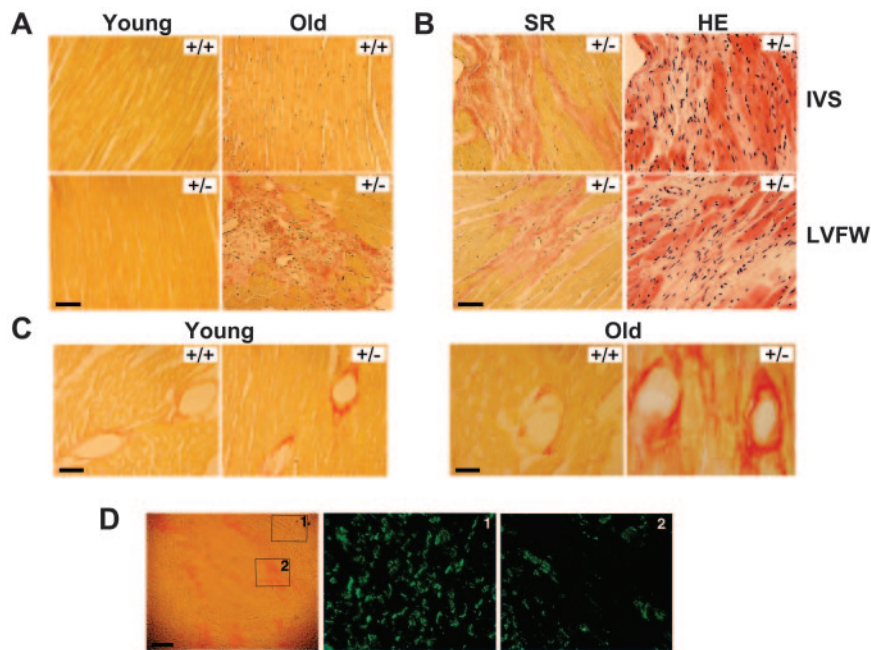


**Figure 3.** Histological sections of ventricular myocardium. A, Sirius red staining of LV from young (14 to 16 weeks; left) and old (right) WT (+/+) and *Scn5a*<sup>+/-</sup> (+/-) mice. Fibrosis appears in red, healthy tissue in yellow. Bar=50  $\mu$ m. B, Fibrosis in old *Scn5a*<sup>+/-</sup> mice. Sirius red (SR; left) and hematoxylin-eosin (HE, right) staining of serial slices taken from interventricular septum (top) and LV free wall (bottom). Bar=50  $\mu$ m. C, Vascular fibrosis in young (left) and old (right) mice. Bar=50  $\mu$ m at left and 25  $\mu$ m at right. D, Low-magnification Sirius red staining of LV of an old *Scn5a*<sup>+/-</sup> mouse showing heterogeneous fibrosis (left). Area 1 shows no fibrosis. Area 2 is fibrotic. Higher magnification of area 1 and 2 immunostained with Connexin43 antibody. Bar=200  $\mu$ m at left and 50  $\mu$ m in high magnification.

concluded that although the distribution of Cx43 in old *Scn5a*<sup>+/-</sup> animals was markedly heterogeneous, its global expression was normal. We simultaneously analyzed the expression of N-cadherin, another intercalated disk-related protein. Surprisingly, this component of the adherence junctions was slightly downregulated in young *Scn5a*<sup>+/-</sup> hearts compared with WT, whereas it was similar in WT and *Scn5a*<sup>+/-</sup> old hearts (Figure 5B).

#### Normal Cardiac Function of Old *Scn5a*<sup>+/-</sup> Mice

Using echocardiography, we assessed the cardiac function in vivo of anesthetized 29- to 30-week-old and 52- to 55-week-old animals. As shown in Table 2, *Scn5a*<sup>+/-</sup> mice exhibited no sign of altered cardiac function and no ventricular hypertrophy. Heart weight-to-body weight ratios of *Scn5a*<sup>+/-</sup> mice did not differ from those of WT mice either at the age of 10 weeks ( $0.49 \pm 0.03$  versus  $0.52 \pm 0.01$  respectively;  $n=8$ ;  $P=NS$ ) or at 50 to 52 weeks ( $0.51 \pm 0.03$  versus  $0.52 \pm 0.02$ ;  $n=7$ ;  $P=NS$ ). Echographic parameters evaluating LV contractility were not different from those of WT mice, including tissue Doppler parameters derived from posterior wall and mitral annulus. Finally, the diastolic LV function was also unaltered (Table 2).

Using Millar catheters, we also evaluated LV pressure, contractility (+dP/dt), and relaxation (-dP/dt). These parameters under baseline conditions were not significantly altered in *Scn5a*<sup>+/-</sup> mice in comparison with WT (Figure 6). The systolic and diastolic blood pressure were also normal (not shown); however, after intravenous challenge with isoproterenol 0.3  $\mu$ g/kg, the contractility was significantly potentialized in WT animals (+dP/dt increased from  $2497 \pm 323$  mm Hg/s to  $2973 \pm 203$  mm Hg/s;  $P<0.05$ ;  $n=5$ ) but not in *Scn5a*<sup>+/-</sup> mice ( $2500 \pm 140$  mm Hg/s versus  $2437 \pm 182$  mm Hg/s;  $n=6$ ). We concluded that the cardiac function of *Scn5a*<sup>+/-</sup> old animals was close to normal.

#### Discussion

The present study demonstrates that mice with targeted disruption of the cardiac main Na<sup>+</sup> channel gene, *Scn5a*, reflect the clinical phenotype of patients with inherited Lenègre's disease, including progressive deterioration of the conduction abnormalities with aging.<sup>4</sup> Our data also show that this phenotype is caused primarily and mostly by a reduced Na<sup>+</sup> current and secondarily by an age-related degenerative process comprising gene expression remodeling and fibrosis as a final outcome of the ionic channel defect. Recently, a family with compound heterozygosity for mutations in *SCN5A* was reported to have a severe form of conduction defect early after birth.<sup>13</sup> Cardiac examination of a patient deceased at the age of 2 years showed ventricular hypertrophy and severe degenerative abnormalities; however, in this family, mutation carriers are expected to have only 5% to 10% of Na current, a situation closer to that of mice with homozygous disruption of *Scn5a*. Defect in another ion channel, the type II ryanodine receptor (RyR2), was also shown to underlie arrhythmogenic right ventricular dysplasia<sup>14</sup>; however, the physiology of RyR2 channels is very different from that of *SCN5A*, because RyR2 is an intracellular protein involved in intracellular Ca<sup>2+</sup> homeostasis.

The configuration of the QRS complex in *Scn5a*<sup>+/-</sup> mice differs from that of WT mice, suggesting abnormal activation of the heart. Therefore, one explanation to connect a decreased Na<sup>+</sup> current and myocardial remodeling could be long-term asynchronous electrical activation of the ventricles leading to abnormal cardiac load. Such a phenomenon was previously reported in dogs submitted to LV pacing at physiological rates.<sup>15</sup> In this model, pacing induced asymmetrical hypertrophy probably related to regional differences in the contraction pattern, without changes on global ventricular performance. Interestingly, although the duration of the QRS complex rapidly doubles immediately after initiating the ventricular pacing, this parameter increases by an additional

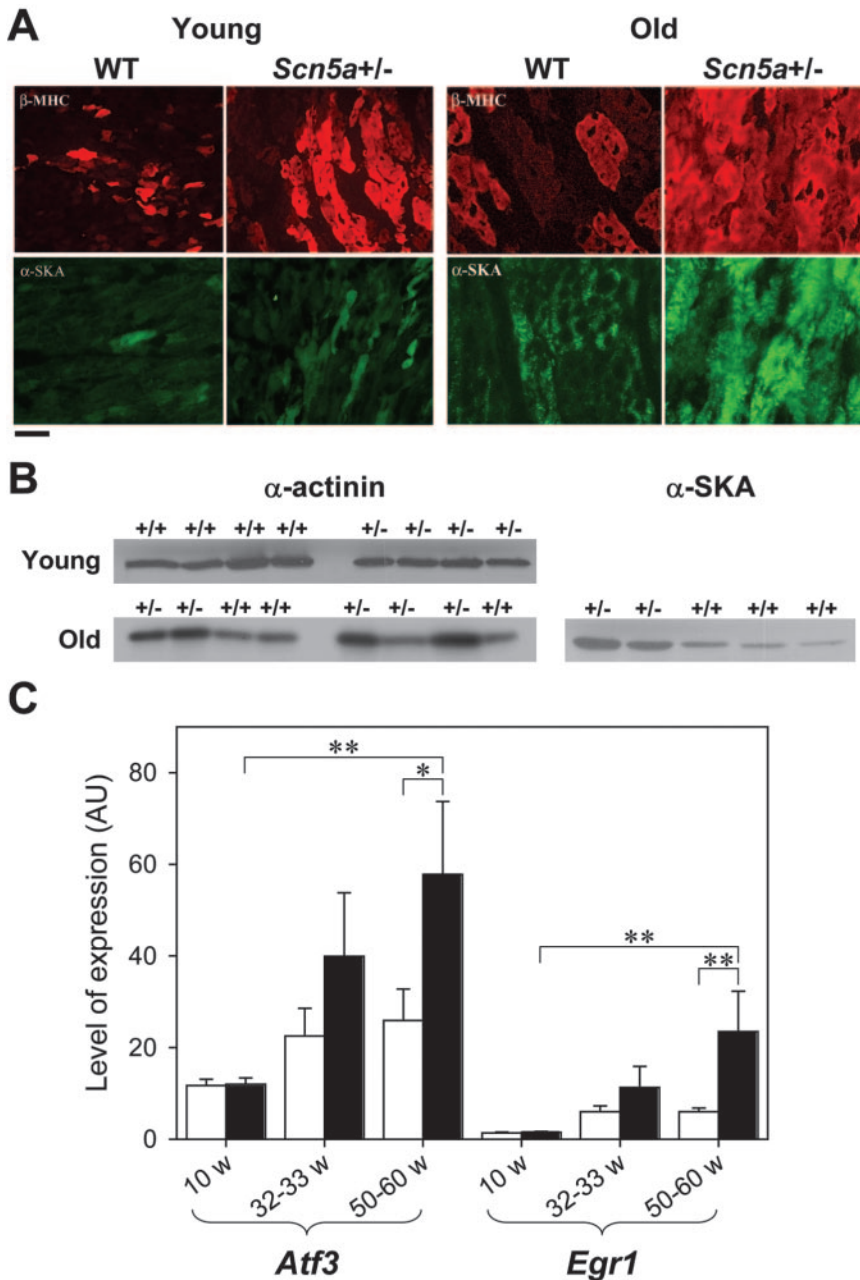


**Figure 4.** Expression of hypertrophic markers in WT and *Scn5a*<sup>+/-</sup> ventricles. A, Immunohistochemical labeling of LV sections from young (14 to 16 weeks) and old (50 to 73 weeks) WT and *Scn5a*<sup>+/-</sup> mice with antibodies against  $\beta$ -MHC ( $\beta$ -MHC; top) and skeletal  $\alpha$ -SKA ( $\alpha$ -SKA; bottom). Level of expression of  $\alpha$ -SKA in young animals was too low for detection. Bar=50  $\mu$ m. B, Representative Western blots showing ventricular expression of  $\alpha$ -actinin and  $\alpha$ -SKA in young and old mice. +/+ is WT; +/- is *Scn5a*<sup>+/-</sup>. Each well was loaded with same amount of protein (30  $\mu$ g; see Methods section for further explanation of loading controls). C, Semiquantitative real-time PCR. Graph represents levels of expression (in arbitrary units) of *Atf3* and *Egr1* genes in WT (open bars) and *Scn5a*<sup>+/-</sup> (filled bars) mice as a function of age (6-, 26-, and 44- to 52-week-old mice). \**P*<0.05; \*\**P*<0.01.

20% after 6 months. In contrast to mice, no fibrosis is observed in these dogs. This may be because of the relatively brief period of abnormal activation and its late initiation during dog life.

In addition to fibrosis, altered expression of connexins might also participate in abnormal conduction in *Scn5a*<sup>+/-</sup> mice. In the mouse heart, 3 different connexins form gap junctions.<sup>16</sup> Cx40 is expressed exclusively in the atrium and the specialized conduction system.<sup>17</sup> In *Scn5a*<sup>+/-</sup> mice, the expression of Cx40 was downregulated in the atria from old mice. Together with decreased Na<sup>+</sup> current, reduced Cx40 might participate in prolonging the P wave. Prolonged P-wave duration is also a common feature of patients with inherited Lenègre's disease.<sup>4</sup> The increased PR interval suggested that Cx40 was also downregulated in the conduction system, although technical difficulties prevented measure-

ment of Cx40 expression in this tissue. Expression of Cx43 was not globally modified but rather locally altered in the regions with marked fibrosis, a phenomenon that may decrease conduction velocity locally and increase the heterogeneity of propagation.<sup>10</sup>

In the mouse model, myocardial rearrangements occurred concomitantly with overexpression of *Atf3*, a member of the CREB/ATF family of transcription factor genes. *Atf3* is normally expressed at very low levels in the heart but is activated by stressors, such as ischemia-reperfusion. This gene seems to play a detrimental role in the pathogenesis of stress-associated cardiac diseases. Interestingly, overexpression of *ATF3* in the mouse heart was previously shown to increase  $\alpha$ -skeletal actin and  $\beta$ -MHC expression and also to induce fibrosis and conduction abnormalities.<sup>18</sup> Because *Atf3* expression increases progressively with age in *Scn5a*<sup>+/-</sup> mice,

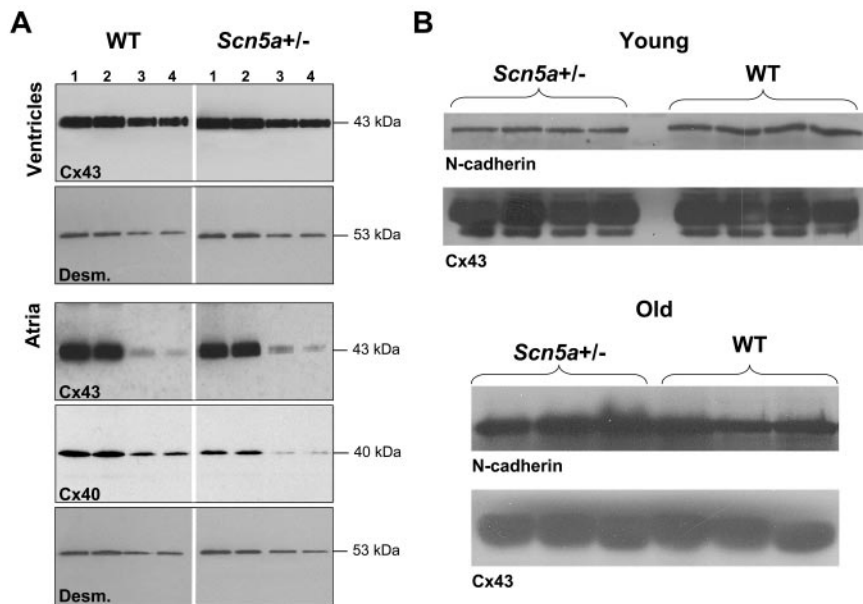


**Figure 5.** Western blot experiments for connexin 40 (Cx40) and 43 (Cx43) expression. A, Representative blots probed with anti-Cx43 or anti-Cx40 antibodies in ventricular and atrial tissues collected from 36- to 48-week-old WT and *Scn5a*<sup>+/-</sup> mice. Intensity of signals obtained after treatment with anti-desmin antibody (Desm.) indicated that similar amounts of protein were loaded in wells 1 and 2 (40  $\mu$ g) and 3 and 4 (20  $\mu$ g). Molecular mass of detected proteins is indicated on right. B, Representative Western blots showing ventricular expression of N-cadherin and Cx43 in young (14 to 16 weeks; top) and old (50 to 73 weeks; bottom) mice. Each well was loaded with same amount of protein (30  $\mu$ g; see Methods section for further explanation of loading controls).

it may represent an important trigger for myocardial remodeling. *Egr1*, an early growth response gene, was also associated with the age-related cardiac remodeling in *Scn5a*<sup>+/-</sup> mice. *Egr1* may positively regulate the expression of  $\alpha$ -skeletal actin and  $\beta$ -MHC, because these proteins are no longer overexpressed during adrenoceptor-induced cardiac

**TABLE 2. Mouse Phenotyping With Echocardiography**

Genotype	Age			
	31 Weeks		52 Weeks	
	WT (n=6)	<i>Scn5a</i> <sup>+/-</sup> (n=7)	WT (n=4)	<i>Scn5a</i> <sup>+/-</sup> (n=8)
HR, bpm	547 $\pm$ 13	525 $\pm$ 5	539 $\pm$ 17	544 $\pm$ 7
BW, g	23.7 $\pm$ 0.9	24.4 $\pm$ 1.4	24.3 $\pm$ 1.0	22.9 $\pm$ 0.5
Remodeling and hypertrophy				
LA, mm	2.65 $\pm$ 0.11	2.42 $\pm$ 0.19	2.35 $\pm$ 0.12	2.42 $\pm$ 0.12
LVEDD, mm	3.94 $\pm$ 0.17	3.38 $\pm$ 0.28	3.99 $\pm$ 0.21	3.60 $\pm$ 0.09
LV/BW, mg/g	4.44 $\pm$ 0.26	4.69 $\pm$ 0.46	3.87 $\pm$ 0.27	3.83 $\pm$ 0.23
LV systolic function				
EF, %	85 $\pm$ 2	84 $\pm$ 3	76 $\pm$ 1	83 $\pm$ 3
VcFc, circ/s	3.09 $\pm$ 0.17	3.32 $\pm$ 0.25	2.77 $\pm$ 0.18	3.53 $\pm$ 0.21
Sa, cm/s	3.01 $\pm$ 0.11	2.96 $\pm$ 0.07	2.46 $\pm$ 0.27	2.49 $\pm$ 0.04
Spw, cm/s	3.22 $\pm$ 0.22	2.99 $\pm$ 0.18	3.04 $\pm$ 0.20	3.03 $\pm$ 0.16
LV diastolic function				
IVRT, ms	15.0 $\pm$ 0.9	14.3 $\pm$ 0.8	16.0 $\pm$ 0.7	15.8 $\pm$ 0.5
E/Ea	18.2 $\pm$ 1.1	18.3 $\pm$ 1.0	20.8 $\pm$ 3.8	16.3 $\pm$ 1.0

HR indicates heart rate; BW, body weight; LA, left atrial dimension; LVEDD, left ventricular end-diastolic diameter; LV/BW, ratio of left ventricular mass to body weight; EF, ejection fraction; VcFc, mean velocity of circumferential fiber shortening corrected for heart rate; Sa, maximal systolic velocity of the mitral annulus; Spw, maximal systolic velocity of the posterior wall; IVRT, isovolumic relaxation time; and E/Ea, ratio of the maximal blood velocity of early LV inflow to the maximal velocity of early diastolic motion of the mitral annulus.

Data are expressed as mean $\pm$ SEM.

hypertrophy in *Egr1*-invalidated mice.<sup>19</sup> Obviously, much more work is needed before the role of *Aft3* and *Egr1* in the pathophysiology of *Scn5a* invalidation is clarified. We hypothesize that a 50% reduction in *Scn5a* could create long-term asynchronous electrical activation of the ventricles and abnormal cardiac load. This could alter the expression of regulatory elements such as *Atf3* and *Egr1* and the expression of hypertrophic markers in the absence of patent hypertrophy. This very slow process should ultimately lead to fiber disarray and fibrosis, which would in turn further impair conduction. Future studies will be driven to confirm this sequence.

Other channelopathies, such as the Brugada syndrome, have been associated with loss-of-function mutations in *SCN5A*.<sup>20</sup> The Brugada syndrome is usually considered an early repolarization disease, involving disequilibrium between a prominent transient outward current in the right ventricular subepicardium and a decreased Na<sup>+</sup> current.<sup>21</sup> Although there is convincing experimental evidence to support this hypothesis, an additional involvement of altered conduction in the pathophysiological sequence leading to this complex disease cannot be excluded.<sup>22,23</sup> Indeed, the frontier between the Brugada syndrome and progressive conduction diseases remains unclear, because in the same family, the same mutation can induce both diseases.<sup>24</sup> Whether the pathophysiology of the Brugada syndrome also involves myocardial fibrosis (either diffuse or localized in the upper right ventricle) remains to be established, particularly for the fraction of Brugada patients carrying a *SCN5A* mutation leading to haploinsufficiency.

In the early descriptions of Lenègre and Moreau<sup>1</sup> and Lev,<sup>2</sup> excessive fibrosis was found primarily in the conductive tissue. In the mouse model, fibrosis is found primarily in the ventricular working myocardium. Species and heart size differences could very well account for this discrepancy. There are indeed well-known differences in ventricular activation in the mouse compared with larger mammals. In mice,

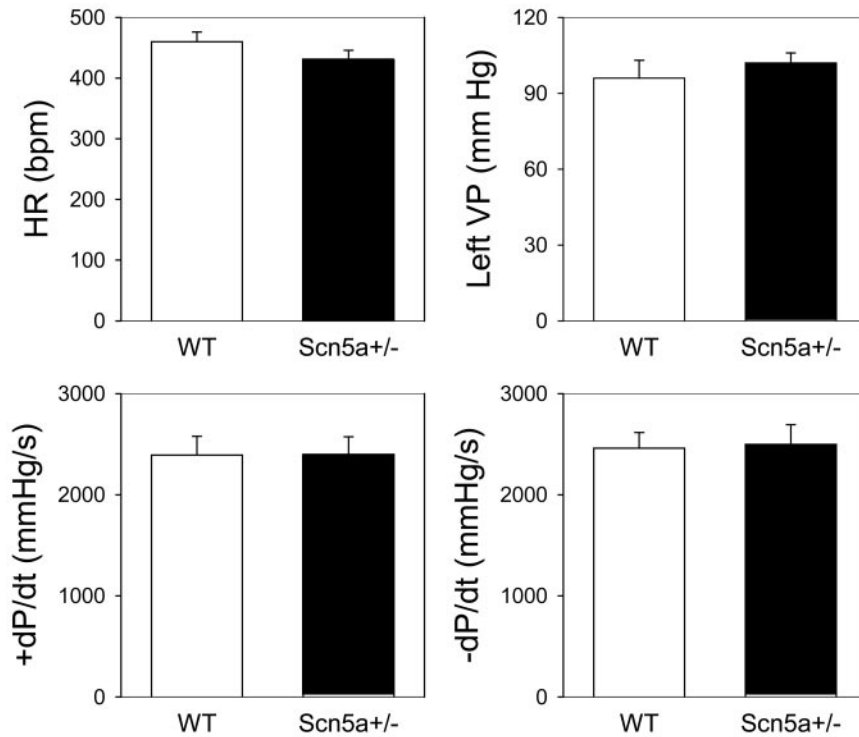


**Figure 6.** Hemodynamics in *Scn5a*<sup>+/-</sup> mice. Heart rate (HR), LV systolic pressure (VP), maximal positive rate of LV pressure development (+dP/dt), and maximal negative rate of LV pressure development (-dP/dt) in WT (n=8; open bars) and *Scn5a*<sup>+/-</sup> (n=7; filled bars) mice.

direct electrical connections are present between the His bundle and upper intraventricular septal regions, whereas the conduction system of larger mammals is electrically insulated from the septal myocardium by a fibrotic sheet.<sup>25</sup> Moreover, conduction velocity in the His bundle branches of the mouse is not faster than in the working myocardium.<sup>12</sup> Another major difference between mouse and human is that the mouse heart contracts 10 times more often per time unit than the human heart. Different cardiac sizes lead to different constraints. That abnormal conduction because of a decreased Na<sup>+</sup> current has slightly different consequences is thus not surprising.

In conclusion, our results obtained in the mouse further support the hypothesis that *SCN5A*-related inherited Lenègre's disease is a result of combined reduced Na<sup>+</sup> current and an age-related channelopathy-mediated increase in fibrosis. Our findings further support the original Lenègre and Lev hypotheses suspecting a fibrotic process to be responsible for slowly progressing atrioventricular blocks and also provide the first univocal demonstration that a monogenic ion channel defect can lead to progressive myocardial structural anomalies with aging.

Finally, on the basis of our data, we plan to evaluate whether antifibrotic drugs such as ACE inhibitors and/or angiotensin II receptor antagonists would prevent the age-related conduction worsening in our mice. A positive outcome would support a pilot clinical trial in hereditary Lenègre's disease and ultimately in idiopathic progressive cardiac conduction disease.

### Acknowledgments

This work was supported by grants from the Ministère de la Recherche (Action Concertée Incitative Biologie du développement et physiologie intégrative; Dr Charpentier), the Groupement d'Intérêt

Scientifique, Institut des Maladies Rares (Dr Charpentier), the Fondation de France (Dr Escande and Dr Gros), the Netherlands Organization for Scientific Research (Dr van Veen), and the British Heart Foundation and the Medical Research Council (Dr Grace). The authors thank Béatrice Le Ray (INSERM U533) for expert technical assistance.

### References

1. Lenègre J, Moreau PH. Le bloc auriculo-ventriculaire chronique: etude anatomique, clinique et histologique. *Arch Mal Cœur*. 1963;56:867-888.
2. Lev M. Anatomic basis for atrioventricular block. *Am J Med*. 1964;37:742-748.
3. Schott JJ, Alshinawi C, Kyndt F, Probst V, Hoorntje TM, Hulsbeek M, Wilde AA, Escande D, Mannens MM, Le Marec H. Cardiac conduction defects associate with mutations in SCN5A. *Nat Genet*. 1999;23:20-21.
4. Probst V, Kyndt F, Potet F, Trochu JN, Mialet G, Demolombe S, Schott JJ, Baró I, Escande D, Le Marec H. Haploinsufficiency in combination with aging causes SCN5A-linked hereditary Lenegre disease. *J Am Coll Cardiol*. 2003;41:643-652.
5. Papadatos GA, Wallerstein PM, Head CE, Ratcliff R, Brady PA, Benndorf K, Saumarez RC, Trezise AE, Huang CL, Vandenberg JI, Colledge WH, Grace AA. Slowed conduction and ventricular tachycardia after targeted disruption of the cardiac sodium channel gene *Scn5a*. *Proc Natl Acad Sci U S A*. 2002;99:6210-6215.
6. Lande G, Demolombe S, Bammert A, Moorman A, Charpentier F, Escande D. Transgenic mice overexpressing human KvLQT1 dominant-negative isoform, II: pharmacological profile. *Cardiovasc Res*. 2001;50:328-334.
7. Mitchell GF, Jeron A, Koren G. Measurement of heart rate and Q-T interval in the conscious mouse. *Am J Physiol*. 1998;274:H747-H751.
8. Livak KJ, Schmittgen TD. Analysis of relative gene expression data using real-time quantitative PCR and the 2(-Delta Delta C(T)) method. *Methods*. 2001;25:402-408.
9. Steenman M, Lamirault G, Le Meur N, Le Cunff M, Escande D, Leger JJ. Distinct molecular portraits of human failing hearts identified by dedicated cDNA microarrays. *Eur J Heart Fail*. 2005;7:157-165.
10. van Veen TA, van Rijen HV, Wiegerinck RF, Ophof T, Colbert MC, Clement S, de Bakker JM, Jongsma HJ. Remodeling of gap junctions in mouse hearts hypertrophied by forced retinoic acid signaling. *J Mol Cell Cardiol*. 2002;34:1411-1423.
11. Sweat F, Puchtler H, Rosenthal SI. Sirius red F3BA as a stain for connective tissue. *Arch Pathol*. 1964;78:69-72.

12. Alcoléa S, Jarry-Guichard T, de Bakker J, Gonzalez D, Lamers W, Coppens S, Barrio L, Jongsma H, Gros D, van Rijen H. Replacement of connexin40 by connexin45 in the mouse: impact on cardiac electrical conduction. *Circ Res*. 2004;94:100–109.
13. Bezzina CR, Rook MB, Groenewegen WA, Herfst LJ, van der Wal AC, Lam J, Jongsma HJ, Wilde AA, Mannens MM. Compound heterozygosity for mutations (W156X and R225W) in SCN5A associated with severe cardiac conduction disturbances and degenerative changes in the conduction system. *Circ Res*. 2003;92:159–168.
14. Tiso N, Stephan DA, Nava A, Bagattin A, Devaney JM, Stanchi F, Larderet G, Brahmbhatt B, Brown K, Bauce B, Muriago M, Basso C, Thiene G, Danieli GA, Rampazzo A. Identification of mutations in the cardiac ryanodine receptor gene in families affected with arrhythmogenic right ventricular cardiomyopathy type 2 (ARVD2). *Hum Mol Genet*. 2001;10:189–194.
15. van Oosterhout MF, Prinzen FW, Arts T, Schreuder JJ, Vanagt WY, Cleutjens JP, Reneman RS. Asynchronous electrical activation induces asymmetrical hypertrophy of the left ventricular wall. *Circulation*. 1998;98:588–595.
16. Gros D, Dupays L, Alcoléa S, Meysen S, Miquerol L, Theveniau-Ruissy M. Genetically modified mice: tools to decode the functions of connexins in the heart: new models for cardiovascular research. *Cardiovasc Res*. 2004;62:299–308.
17. Miquerol L, Meysen S, Mangoni M, Bois P, van Rijen HV, Abran P, Jongsma H, Nargeot J, Gros D. Architectural and functional asymmetry of the His-Purkinje system of the murine heart. *Cardiovasc Res*. 2004;63:77–86.
18. Okamoto Y, Chaves A, Chen J, Kelley R, Jones K, Weed HG, Gardner KL, Gangi L, Yamaguchi M, Klomkleaw W, Nakayama T, Hamlin RL, Carnes C, Altschuld R, Bauer J, Hai T. Transgenic mice with cardiac-specific expression of activating transcription factor 3, a stress-inducible gene, have conduction abnormalities and contractile dysfunction. *Am J Pathol*. 2001;159:639–650.
19. Saadane N, Alpert L, Chalifour LE. Altered molecular response to adrenoceptor-induced cardiac hypertrophy in Egr-1-deficient mice. *Am J Physiol*. 2000;278:H796–H805.
20. Chen Q, Kirsch GE, Zhang D, Brugada R, Brugada J, Brugada P, Potenza D, Moya A, Borggrefe M, Breithardt G, Ortiz-Lopez R, Wang Z, Antzelevitch C, O'Brien RE, Schulze-Bahr E, Keating MT, Towbin JA, Wang Q. Genetic basis and molecular mechanism for idiopathic ventricular fibrillation. *Nature*. 1998;392:293–296.
21. Antzelevitch C, Brugada P, Brugada J, Brugada R, Towbin JA, Nademanee K. Brugada syndrome: 1992–2002: a historical perspective. *J Am Coll Cardiol*. 2003;41:1665–1671.
22. Tukkie R, Sogaard P, Vleugels J, de Groot IK, Wilde AA, Tan HL. Delay in right ventricular activation contributes to Brugada syndrome. *Circulation*. 2004;109:1272–1277.
23. Martini B. Further confirmation that a conduction disturbance underlies the electrocardiographic pattern of the so-called Brugada syndrome. *Circulation*. 2004;110:e53. Letter.
24. Kyndt F, Probst V, Potet F, Demolombe S, Chevallier JC, Baro I, Moisan JP, Boisseau P, Schott JJ, Escande D, Le Marec H. Novel SCN5A mutation leading either to isolated cardiac conduction defect or Brugada syndrome in a large French family. *Circulation*. 2001;104:3081–3086.
25. van Rijen HV, van Veen TA, van Kempen MJ, Wilms-Schopman FJ, Potse M, Krueger O, Willecke K, Opthof T, Jongsma HJ, de Bakker JM. Impaired conduction in the bundle branches of mouse hearts lacking the gap junction protein connexin40. *Circulation*. 2001;103:1591–1598.